Statistical analysis

Comparisons of means between 2 groups were performed using the unpaired Student's *t*-test (for Aβ), while those among the 4 groups were performed with ANOVA (for cholesterol, synaptophysin, and probe trial) or two-factor repeated measures ANOVA (for memory acquisition) followed by Fisher's PLSD test. Differences with a p value of less than 0.05 were considered significant.

Results

Diet-induced hypercholesterolemia in APP_{OSK}-Tg mice

Five-month-old male APP_{OSK}-Tg mice and non-Tg littermates were fed a high-cholesterol diet for 1 month to induce hypercholesterolemia. Control APP_{OSK}-Tg mice and non-Tg littermates were fed normal chow. At the end of the month, serum cholesterol levels of the APP_{OSK}-Tg mice and non-Tg littermates that were fed the high-cholesterol diet were significantly higher than those of their counterparts fed a normal diet (Fig. 1A), indicating that hypercholesterolemia was successfully induced. Brain cholesterol levels in these mice were also measured after behavioral tests. Both hypercholesterolemic APP_{OSK}-Tg mice and hypercholesterolemic non-Tg littermates showed higher cholesterol levels in the hippocampus than control mice (Fig. 1B), although this increase was significant in the APP_{OSK}-Tg mice only.

Cognitive dysfunction in hypercholesterolemic APP_{OSK}-Tg mice

To determine whether hypercholesterolemia affects cognitive function in mice, we studied the spatial reference memory of mice using the Morris water maze when mice were 6 months of age, a time when APP_{OSK}-Tg mice ordinarily show no symptoms or pathology of AD. Mice were trained for 5 days to remember the location of a hidden platform in a swimming pool (memory acquisition), and were tested for memory retention at day 6 in a probe trial with the platform removed. Hypercholesterolemic non-Tg littermates showed performance similar to or slightly better than control non-Tg littermates in both memory acquisition (Fig. 2A) and retention tests (Fig. 2B). Control APP_{OSK}-Tg mice also showed performance similar to or slightly worse than control non-Tg littermates, whereas hypercholesterolemic APP_{OSK}-Tg mice displayed significant deficits in performance with longer escape latencies in the memory acquisition test and lower time occupancy in the target quadrant in the probe trial than control non-Tg littermates. These results indicate that hypercholesterolemia does not significantly affect cognitive function in wild-type mice at 6 months of age, but causes earlier onset of memory impairment in APP_{OSK}-Tg mice. After the water maze task, locomotor activities of mice were examined by an open field test. No significant difference in locomotion among the 4 groups was recorded (data not shown), indicating that the memory impairment observed in hypercholesterolemic APP_{OSK}-Tg mice was not due to motor dysfunction.

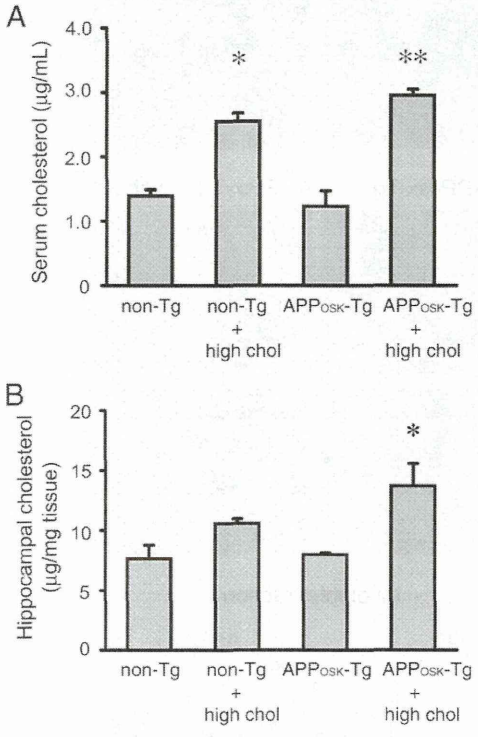

Fig. 1. Serum and brain cholesterol levels in mice. Five-month-old APP_{OSK}-Tg mice and non-Tg littermates were fed a high-cholesterol diet or normal chow for 1 month. (A) Serum cholesterol levels were determined before behavioral tests. The results are means ± S.E.M. (n = 5 for hypercholesterolemic APP_{OSK}-Tg mice; n = 8 for other groups). *p < 0.0001 vs non-Tg littermates fed normal chow; p < 0.0001 vs APP_{OSK}-Tg mice fed normal chow; not significant vs APP_{OSK}-Tg mice fed high-cholesterol diet, **p < 0.0001 vs non-Tg littermates fed normal chow; p < 0.0001 vs APP_{OSK}-Tg mice fed normal chow. (B) Brain cholesterol levels were determined from the hippocampal tissues after behavioral tests. The results are means ± S.E.M. (n = 3 per group). *p = 0.0031 vs non-Tg littermates fed normal chow; p = 0.0043 vs APP_{OSK}-Tg mice fed normal chow; not significant vs non-Tg littermates fed high-cholesterol diet.

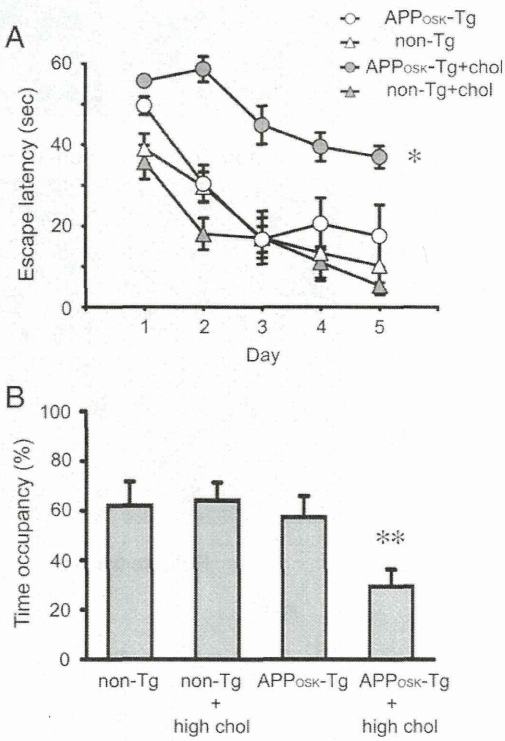

Fig. 2. Memory impairment in hypercholesterolemic APP_{OSK}-Tg mice. Six-month-old APP_{OSK}-Tg mice and non-Tg littermates with or without hypercholesterolemia were tested for spatial reference memory. Memory acquisition (A) and retention (B) were assessed using the Morris water maze. In probe trials (B), time spent in the target quadrant was measured. The results are means ± S.E.M. (n = 5 for hypercholesterolemic APP_{OSK}-Tg mice; n = 8 for other groups). *p < 0.0001 vs normal non-Tg littermates; p < 0.0001 vs hypercholesterolemic non-Tg littermates; p = 0.0003 vs normal APP_{OSK}-Tg mice, **p = 0.0209 vs normal non-Tg littermates; p = 0.0148 vs hypercholesterolemic non-Tg littermates; p = 0.0443 vs normal APP_{OSK}-Tg mice.

Intraneuronal accumulation of Aβ oligomers in hypercholesterolemic APP_{OSK}-Tg mice

We previously showed that cognitive dysfunction in APP_{OSK}-Tg mice was associated with intraneuronal accumulation of Aβ oligomers and subsequent synapse loss (Tomiyama et al., 2010). To investigate the effect of hypercholesterolemia on intraneuronal Aβ, we examined the brain sections of mice by immunohistochemistry using β001 antibody that recognizes the N-terminus of Aβ and NU-1 antibody that selectively recognizes Aβ oligomers. Sections from control non-Tg littermates, control APP_{OSK}-Tg mice and hypercholesterolemic non-Tg littermates were negative for staining with β001 (Fig. 3A) and NU-1 (Fig. 3B) in the hippocampus and cerebral cortex. In contrast, hypercholesterolemic APP_{OSK}-Tg mice exhibited marked staining with β001 and NU-1 within neurons in the hippocampal CA3 region and some staining in the cerebral cortex at 6 months of age. In our previous observation, these brain regions showed Aβ oligomer accumulation only from 8 months of age in APP_{OSK}-Tg mice (Tomiyama et al., 2010). Thus, hypercholesterolemia accelerated accumulation of intraneuronal Aβ oligomers in APP_{OSK}-Tg mice. Hypercholesterolemia-induced accumulation of brain Aβ was confirmed by ELISA. The levels of Aβ1-40 and Aβ1-42 in TBS soluble fractions were significantly increased in hypercholesterolemic APP_{OSK}-Tg mice, compared with control APP_{OSK}-Tg mice (Fig. 3C). TBS insoluble Aβ1-40 and Aβ1-42 were also increased, although the changes were not significant.

Synapse loss in hypercholesterolemic APP_{OSK}-Tg mice

We next examined whether synapse loss also occurred in hypercholesterolemic APP_{OSK}-Tg mice at 6 months of age. Brain sections were stained with an antibody to the presynaptic marker synaptophysin and the intensities were quantified. Neither control APP_{OSK}-Tg mice nor hypercholesterolemic non-Tg littermates showed significant changes in synaptophysin levels in the hippocampus compared with control non-Tg littermates (Fig. 4A and B). In contrast, hypercholesterolemic APP_{OSK}-Tg mice displayed a marked decrease in synaptophysin

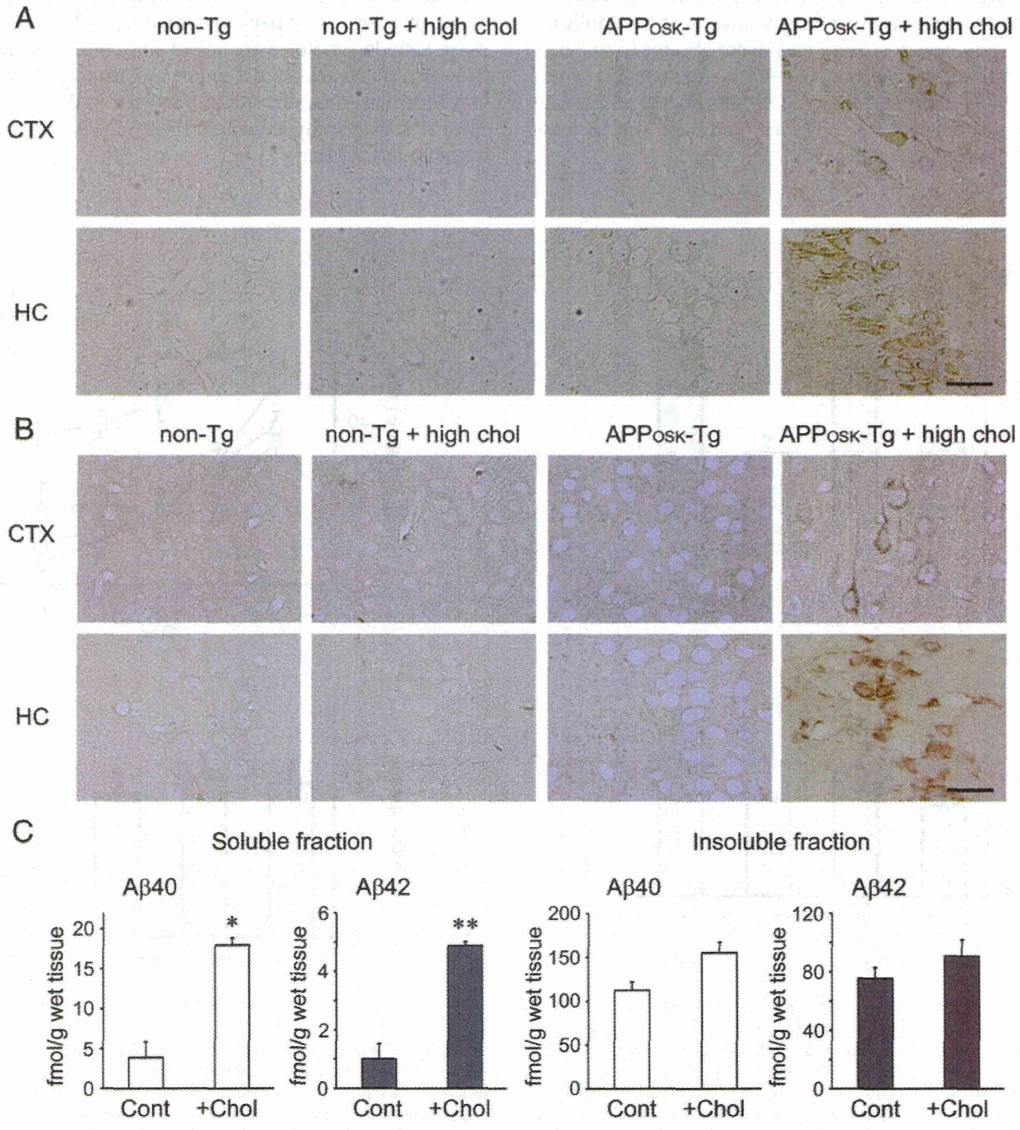

Fig. 3. Intraneuronal accumulation of Aβ oligomers in hypercholesterolemic APP_{OSK}-Tg mice. Brain sections from 6-month-old APP_{OSK}-Tg mice and non-Tg littermates with or without hypercholesterolemia were stained with antibodies to Aβ (β001, A) and Aβ oligomers (NU-1, B). The photographs show the cerebral cortex (CTX) and hippocampal CA3 regions (HC). Scale bar = 30 μm. (C) Aβ concentrations in brain TBS soluble and insoluble fractions from APP_{OSK}-Tg mice with or without hypercholesterolemia were measured by ELISA. The results are means ± S.E.M. (n = 3 per group). *p = 0.0019 and **p = 0.0020 vs control APP_{OSK}-Tg mice.

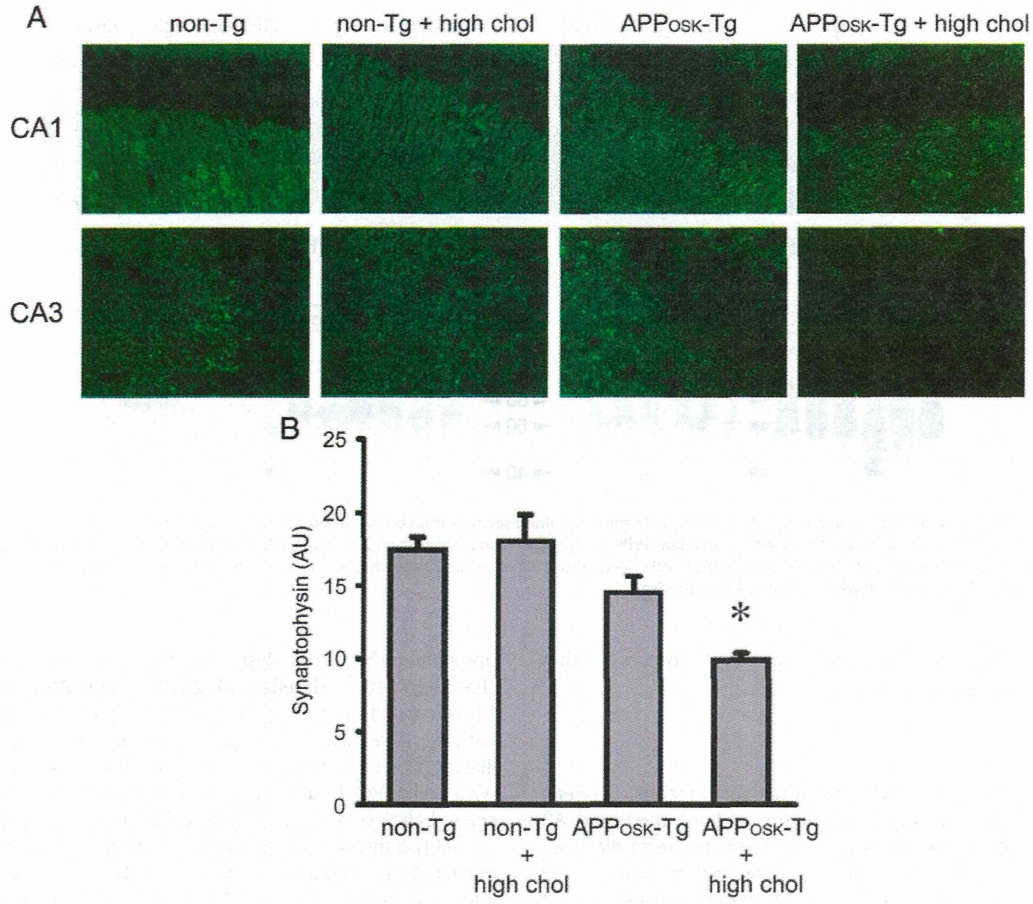

Fig. 4. Decrease in synaptophysin levels in hypercholesterolemic APP_{OSK}-Tg mice. (A) Brain sections from 6-month-old APP_{OSK}-Tg mice and non-Tg littermates with or without hypercholesterolemia were stained with antibody to synaptophysin. The photographs show the hippocampal CA1 and CA3 regions. (B) The synaptophysin fluorescence intensities in the hippocampal CA3 regions were quantified and shown in arbitrary units (AU). The results are means ± S.E.M. ($n = 3$ per group). *$p = 0.0019$ vs normal non-Tg littermates; $p = 0.0012$ vs hypercholesterolemic non-Tg littermates; $p = 0.0239$ vs normal APP_{OSK}-Tg mice.

levels in the hippocampus. Again, since our previous study showed that hippocampal synapse loss in APP_{OSK}-Tg mice occurred from 8 months of age (Tomiyama et al., 2010), this collectively indicates that hypercholesterolemia also accelerated synaptic alteration.

Abnormal tau phosphorylation in hypercholesterolemic APP_{OSK}-Tg mice

Our previous study revealed that APP_{OSK}-Tg mice developed abnormal tau phosphorylation soon after the beginning of intraneuronal accumulation of Aβ oligomers (Tomiyama et al., 2010). It is of interest to clarify whether hypercholesterolemia also accelerates tau pathology. Brain sections were stained with PHF-1, an antibody to phosphorylated tau. Control and hypercholesterolemic non-Tg littermates and control APP_{OSK}-Tg mice displayed no staining in the hippocampus and cerebral cortex (Fig. 5A). In contrast, hypercholesterolemic APP_{OSK}-Tg mice exhibited PHF-1-positive staining in hippocampal Mossy fibers at 6 months of age. These results indicate that hypercholesterolemia accelerated not only Aβ but also tau pathology, and that the latter pathology was probably mediated by intraneuronal Aβ oligomers, not directly by hypercholesterolemia itself. Hypercholesterolemia-accelerated abnormal tau phosphorylation was confirmed by western blot. While total tau levels did not differ between hypercholesterolemic and control APP_{OSK}-Tg mice, the levels of PHF-1-positive phosphorylated tau were apparently increased in hypercholesterolemic APP_{OSK}-Tg mice in both TBS soluble and insoluble fractions (Fig. 5B).

Hypercholesterolemia-accelerated intraneuronal Aβ oligomers in Tg2576 mice

Aβ with the Osaka (E22Δ) mutation has a particular tendency to accumulate within cells, forming oligomers in contrast to wild-type Aβ (Nishitsuji et al., 2009; Ito et al., 2009; Tomiyama et al., 2010; Umeda et al., 2011). This raises the question of whether or not other mouse models expressing wild-type Aβ also show hypercholesterolemia-accelerated accumulation of intraneuronal Aβ oligomers as we observed in APP_{OSK}-Tg mice. To address this question, we examined the effect of hypercholesterolemia on intraneuronal Aβ oligomers in a well-known AD model mouse, Tg2576. This mouse has been reported to start amyloid deposition from 9 to 10 months of age (Hsiao et al., 1996). We fed 7-month-old Tg2576 mice the high-cholesterol diet for 1 month and examined their amyloid pathology at 8 months of age by immunohistochemistry. Control Tg2576 mice that were fed normal chow showed intracellular β001- and NU-1-positive staining in the cerebral cortex and rarely in the hippocampus but no extracellular amyloid deposition (Fig. 6A and B). On the other hand, Tg2576 mice that were fed the high-cholesterol diet exhibited intensely intracellular β001- and NU-1-positive staining in both the cerebral cortex and hippocampus, and furthermore, a few extracellular amyloid deposits in the cerebral cortex and entorhinal cortex (Fig. 6C). Notably, some of these deposits were tiny, atypical in morphology, and closely associated with neuronal cell bodies as if they had overflowed the cells. These results indicate that hypercholesterolemia-accelerated accumulation of intraneuronal Aβ

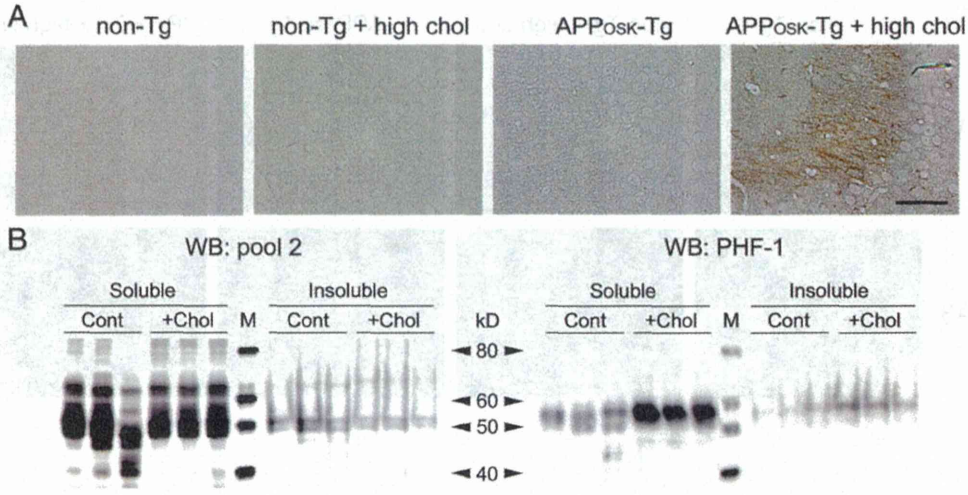

Fig. 5. Abnormal tau phosphorylation in hypercholesterolemic APP_{OSK}-Tg mice. (A) Brain sections from 6-month-old APP_{OSK}-Tg mice and non-Tg littermates with or without hypercholesterolemia were stained with antibody to phosphorylated tau (PHF-1). The photographs show the hippocampal CA3 regions. Scale bar = 50 μm. (B) The levels of total and phosphorylated tau in brain TBS soluble and insoluble fractions from APP_{OSK}-Tg mice with or without hypercholesterolemia were examined by western blot using pool 2 and PHF-1 antibodies, respectively. M, MagicMark XP western standard (Invitrogen).

oligomers is not restricted to APP_{OSK}-Tg mice but also occurs in other model mice.

Discussion

In the present study, we investigated the relationships between hypercholesterolemia, memory impairment, and intraneuronal Aβ using our AD model mouse, APP_{OSK}-Tg. A high-cholesterol diet successfully induced hypercholesterolemia in normal and AD model mice. Brain cholesterol levels were also increased, suggesting that they reflect the levels of serum cholesterol. It is generally believed that cholesterol itself does not easily cross the blood brain barrier and that brain and peripheral cholesterol levels are independently regulated. However, brain cholesterol can be excreted into the circulation via its conversion into 24S-hydroxycholesterol, and inversely, peripheral cholesterol can be taken up by the brain via its conversion into 27-hydroxycholesterol (**Björkhem, 2006**). These transports are presumed to occur by diffusion due to the concentration gradient of each oxysterol between the brain and the circulation (**Björkhem, 2006**). Thus, high levels of serum cholesterol may cause an increased flux of cholesterol from the circulation into the brain through the conversion between cholesterol and oxysterol, leading to increased levels of brain cholesterol. We found that hypercholesterolemia accelerates intraneuronal accumulation of Aβ oligomers and subsequent synapse loss resulting in memory impairment. Control APP_{OSK}-Tg mice that were fed normal chow showed neither intraneuronal Aβ oligomers nor memory impairment at the same age (6 months old). Our findings suggest that intraneuronal Aβ, particularly its oligomeric forms, play an important role in the onset of cognitive dysfunction in AD.

It has been shown that high levels of cellular cholesterol inhibit α-secretase (**Bodovitz and Klein, 1996**) and increase Aβ generation via activation of both β- and γ-secretases (**Frears et al., 1999; Xiong et al., 2008**) and that diet-induced hypercholesterolemia increases Aβ levels in the brain and thus accelerates extracellular Aβ deposition in transgenic mice (**Refolo et al., 2000; Shie et al., 2002**). The present study shows that diet-induced hypercholesterolemia also enhances the intraneuronal accumulation of Aβ in both APP_{OSK}-Tg and Tg2576 mice. Aβ is generated in various intracellular compartments such as the ER, Golgi apparatus, endosomes, and autophagosomes, in addition to the plasma membrane (**Nishitsuji et al., 2009**). Enhanced Aβ generation in these organelles stimulated by high cholesterol intake would result in intracellular accumulation of Aβ. We previously proposed that Aβ upregulation by high cholesterol stimulation occurs to maintain cellular cholesterol levels (**Umeda et al., 2010**). That is, Aβ mediates cholesterol efflux from cells by forming high-density lipoprotein (HDL)-like particles with excess cellular cholesterol during its secretion. This apolipoprotein-like function of Aβ requires interaction with ATP-binding cassette transporter A1 (ABCA1), a transmembrane protein as a cholesterol donor. In general, cholesterol is taken up by cells via receptor-mediated endocytosis and is transported from endosomes to the ER and the plasma membranes. Thus, increased levels of cellular cholesterol may promote interaction between Aβ and ABCA1 within the plasma membrane or intracellular compartments such as endosomes and ER, which may lead to intracellular accumulation of Aβ. It has also been proposed that Aβ regulates cellular cholesterol levels by inhibiting the cholesterol biosynthesis enzyme, hydroxymethylglutaryl-CoA (HMG-CoA) reductase (**Grimm et al., 2005**). Since this enzyme primarily localizes to the ER, the Aβ produced in response to high levels of cellular cholesterol may accumulate in the ER to inhibit further cholesterol synthesis.

The mechanism underlying intraneuronal Aβ-induced memory impairment remains unclear. We have investigated the mechanisms by which intraneuronal accumulation of Aβ oligomers cause cell death in APP_{OSK}-Tg mice (**Umeda et al., 2011**). Aβ oligomers accumulated within the ER, endosomes/lysosomes, and mitochondria in hippocampal neurons of APP_{OSK}-Tg mice and caused ER stress, endosomal/lysosomal leakage, and mitochondrial dysfunction at 18 months of age. These insults presumably lead to eventual neuronal death, i.e. at 24 months of age in APP_{OSK}-Tg mice. At younger ages, the damage caused by intracellular Aβ oligomers would be less, but even mild aberration in these organelles might profoundly affect synaptic function, because these organelles play crucial roles in cellular Ca^{2+} control and endocytosis/exocytosis, which are both involved in synaptic function. In addition, APP_{OSK}-Tg mice were demonstrated to develop abnormal tau phosphorylation soon after the beginning of intraneuronal accumulation of Aβ oligomers (**Tomiyama et al., 2010**), suggesting that intraneuronal Aβ oligomers trigger the pathological alteration of tau. Abnormal phosphorylation of tau would affect its function in axonal transport and in dendrites, leading to synaptic dysfunction. Hippocampal neurons in culture respond to toxic Aβ oligomers with increased tau phosphorylation (**De Felice et al., 2008**) and impaired axonal transport (**Decker et al., 2010**). Hypercholesterolemia is presumed to accelerate these synaptotoxic processes by enhancing Aβ generation.

In this study, we observed the very beginning of amyloid plaque formation in 8-month-old hypercholesterolemic Tg2576 mice, at

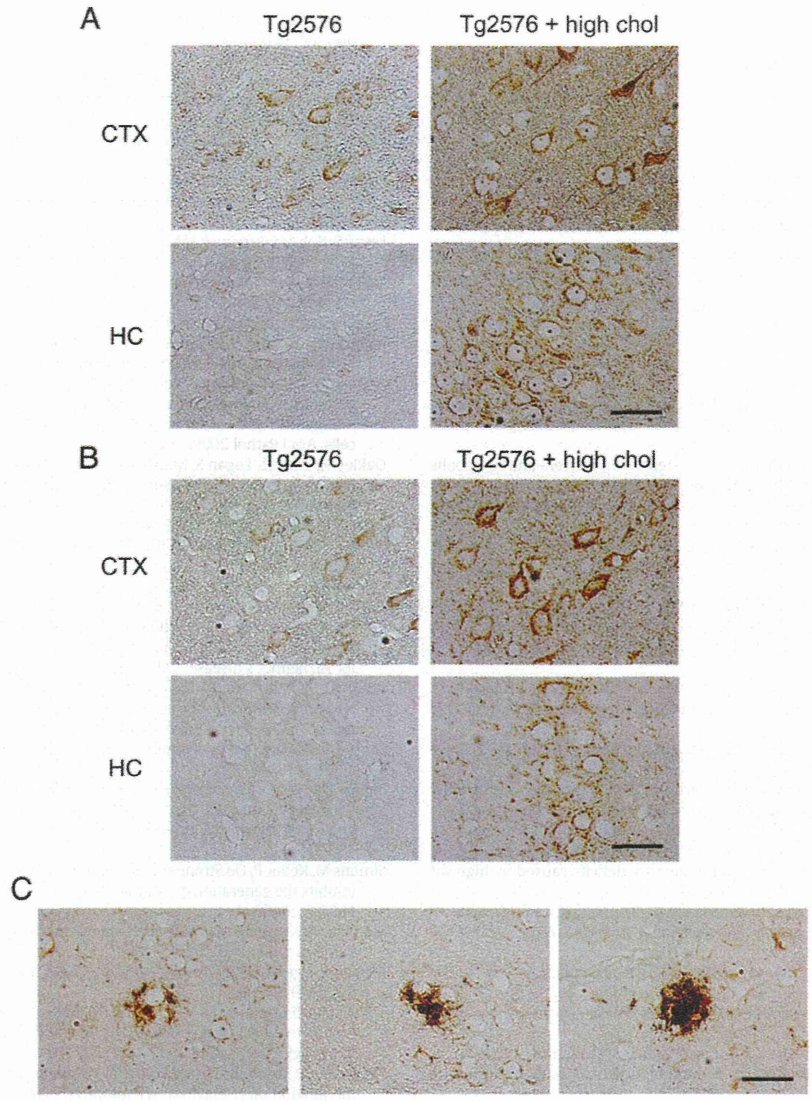

Fig. 6. Intraneuronal accumulation of Aβ oligomers in hypercholesterolemic Tg2576 mice. Seven-month-old Tg2576 mice were fed a high-cholesterol diet or normal chow for 1 month. Their brain sections were stained with antibodies to Aβ (β001, A and C) and Aβ oligomers (NU-1, B). (A, B) The photographs show the cerebral cortex (CTX) and hippocampal CA3 regions (HC). (C) Extracellular amyloid deposits were detected in the cerebral cortex and entorhinal cortex of hypercholesterolemic mice. Scale bar = 30 μm.

which age intraneuronal accumulation of Aβ was already detected, even in normal Tg2576 mice. It is noteworthy that some of these extracellular Aβ deposits were closely associated with neuronal cell bodies, implying the possibility that they originated from intracellular Aβ pools. Similar observations have been reported in AD patients (**D'Andrea et al., 2001**) and other mouse models (**Oakley et al., 2006**). In addition, previous studies have suggested that intraneuronal Aβ serves as a source for extracellular amyloid deposits (**Oddo et al., 2006**) and that amyloid seeds are formed by intracellular concentration and aggregation of Aβ within endosomal/lysosomal compartments (**Hu et al., 2009; Friedrich et al., 2010**). Taken together, it is likely that enhanced accumulation of intraneuronal Aβ and its subsequent leakage from cells into the extracellular space during neurodegenerative processes led to the accelerated extracellular amyloid deposition in hypercholesterolemic mice (**Refolo et al., 2000; Shie et al., 2002**; and the present study).

Our findings imply that intracellular Aβ oligomers play important roles in synaptic and cognitive dysfunction. However, we cannot exclude the possibility that both extracellular and intracellular Aβ oligomers contribute to the synaptic pathology of AD. For example, Tg2576 mice have been reported to exhibit memory impairment at 6 months of age accompanied with the appearance of extracellular soluble Aβ oligomers termed Aβ56 (**Lesné et al., 2006**). On the other hand, we detected intraneuronal accumulation of Aβ in Tg2576 mice at the same age (6-month-old) using human Aβ-specific monoclonal antibody 82E1, although the immunoreactivities were very faint (unpublished observation). In APP_{OSK}-Tg mice and 3xTg-AD mice, memory impairment appeared to be closely correlated with intraneuronal Aβ accumulation. Nevertheless, further studies are required to elucidate the possible existence of extracellular synaptotoxic Aβ species associated with memory impairment in these mice.

Conclusion

Diet-induced hypercholesterolemia in APP_{OSK}-Tg mice caused earlier onset of cognitive dysfunction, which was accompanied with accelerated accumulation of intraneuronal Aβ oligomers and subsequent synapse loss in the hippocampus. Our findings suggest that hypercholesterolemia causes memory impairment by accelerating intraneuronal accumulation of Aβ, particularly its oligomeric form.

Conflict of interest statement

The authors declare that there are no conflicts of interest.

Acknowledgments

This study was supported by the Grants-in-Aid for Scientific Research from the Ministry of Education, Culture, Sports, Science and Technology of Japan (nos. 21500352, 20023026, 21390271, 20023027, 18023033, 17300114); by the Grants-in-Aid for Comprehensive Research on Dementia from the Ministry of Health, Labour, and Welfare, Japan; and in part by the Alzheimer's Association (IIRG-09-132098).

References

Billings LM, Oddo S, Green KN, McGaugh JL, LaFerla FM. Intraneuronal Aβ causes the onset of early Alzheimer's disease-related cognitive deficits in transgenic mice. Neuron 2005;45:675–88.

Björkhem I. Crossing the barrier: oxysterols as cholesterol transporters and metabolic modulators in the brain. J Intern Med 2006;260:493–508.

Bodovitz S, Klein WL. Cholesterol modulates α-secretase cleavage of amyloid precursor protein. J Biol Chem 1996;271:4436–40.

D'Andrea MR, Nagele RG, Wang HY, Peterson PA, Lee DH. Evidence that neurones accumulating amyloid can undergo lysis to form amyloid plaques in Alzheimer's disease. Histopathology 2001;38:120–34.

Decker H, Lo KY, Unger SM, Ferreira ST, Silverman MA. Amyloid-β peptide oligomers disrupt axonal transport through an NMDA receptor-dependent mechanism that is mediated by glycogen synthase kinase 3β in primary cultured hippocampal neurons. J Neurosci 2010;30:9166–71.

De Felice FG, Wu D, Lambert MP, Fernandez SJ, Velasco PT, Lacor PN, et al. Alzheimer's disease-type neuronal tau hyperphosphorylation induced by Aβ oligomers. Neurobiol Aging 2008;29:1334–47.

Endoh R, Ogawara M, Iwatsubo T, Nakano I, Mori H. Lack of the carboxyl terminal sequence of tau in ghost tangles of Alzheimer's disease. Brain Res 1993;601:164–72.

Fernández-Vizarra P, Fernández AP, Castro-Blanco S, Serrano J, Bentura ML, Martínez-Murillo R, et al. Intra- and extracellular Aβ and PHF in clinically evaluated cases of Alzheimer's disease. Histol Histopathol 2004;19:823–44.

Fitz NF, Cronican A, Pham T, Fogg A, Fauq AH, Chapman R, et al. Liver X receptor agonist treatment ameliorates amyloid pathology and memory deficits caused by high-fat diet in APP23 mice. J Neurosci 2010;30:6862–72.

Friedrich RP, Tepper K, Rönicke R, Soom M, Westermann M, Reymann K, et al. Mechanism of amyloid plaque formation suggests an intracellular basis of Aβ pathogenicity. Proc Natl Acad Sci U S A 2010;107:1942–7.

Frears ER, Stephens DJ, Walters CE, Davies H, Austen BM. The role of cholesterol in the biosynthesis of β-amyloid. Neuroreport 1999;10:1699–705.

Gouras GK, Tsai J, Naslund J, Vincent B, Edgar M, Checler F, et al. Intraneuronal Aβ42 accumulation in human brain. Am J Pathol 2000;156:15–20.

Gouras GK, Tampellini D, Takahashi RH, Capetillo-Zarate E. Intraneuronal β-amyloid accumulation and synapse pathology in Alzheimer's disease. Acta Neuropathol 2010;119:523–41.

Greenberg SG, Davies P, Schein JD, Binder LI. Hydrofluoric acid-treated τ_{PHF} proteins display the same biochemical properties as normal τ. J Biol Chem 1992;267:564–9.

Grimm MOW, Grimm HS, Pätzold AJ, Zinser EG, Halonen R, Duering M, et al. Regulation of cholesterol and sphingomyelin metabolism by amyloid-β and presenilin. Nature Cell Biol 2005;7:1118–23.

Grimm MOW, Grimm HS, Tomic I, Beyreuther K, Hartmann T, Bergmann C. Independent inhibition of Alzheimer disease β- and γ-secretase cleavage by lowered cholesterol levels. J Biol Chem 2008;283:11302–11.

Gyure KA, Durham R, Stewart WF, Smialek JE, Troncoso JC. Intraneuronal Aβ-amyloid precedes development of amyloid plaques in Down syndrome. Arch Pathol Lab Med 2001;125:489–92.

Hsiao K, Chapman P, Nilsen S, Eckman C, Harigaya Y, Younkin S, et al. Correlative memory deficits, Aβ elevation, and amyloid plaques in transgenic mice. Science 1996;274:99–102.

Hu X, Crick SL, Bu G, Frieden C, Pappu RV, Lee JM. Amyloid seeds formed by cellular uptake, concentration, and aggregation of the amyloid-β peptide. Proc Natl Acad Sci U S A 2009;106:20324–9.

Ishibashi K, Tomiyama T, Nishitsuji K, Hara M, Mori H. Absence of synaptophysin near cortical neurons containing oligomer Aβ in Alzheimer's disease brain. J Neurosci Res 2006;84:632–6.

Ito K, Ishibashi K, Tomiyama T, Umeda T, Yamamoto K, Kitajima E, et al. Oligomeric amyloid β-protein as a therapeutic target in Alzheimer's disease: its significance based on its distinct localization and the occurrence of a familial variant form. Curr Alzheimer Res 2009;6:132–6.

Klein WL, Krafft GA, Finch CE. Targeting small Aβ oligomers: the solution to an Alzheimer's disease conundrum? Trends Neurosci 2001;24:219–24.

Knobloch M, Konietzko U, Krebs DC, Nitsch RM. Intracellular Abeta and cognitive deficits precede beta-amyloid deposition in transgenic arcAbeta mice. Neurobiol Aging 2007;28:1297–306.

Kurata T, Miyazaki K, Kozuki M, Panin VL, Morimoto N, Ohta Y, et al. Atorvastatin and pitavastatin improve cognitive function and reduce senile plaque and phosphorylated tau in aged APP mice. Brain Res 2011;1371:161–70.

LaFerla FM, Green KN, Oddo S. Intracellular amyloid-β in Alzheimer's disease. Nat Rev Neurosci 2007;8:499–509.

Lambert MP, Velasco PT, Chang L, Viola KL, Fernandez S, Lacor PN, et al. Monoclonal antibodies that target pathological assemblies of Aβ. J Neurochem 2007;100:23–35.

Lesné S, Koh MT, Kotilinek L, Kayed R, Glabe CG, Yang A, et al. A specific amyloid-β protein assembly in the brain impairs memory. Nature 2006;440:352–7.

Lippa CF, Ozawa K, Mann DM, Ishii K, Smith TW, Arawaka S, et al. Deposition of β-amyloid subtypes 40 and 42 differentiates dementia with Lewy bodies from Alzheimer disease. Arch Neurol 1999;56:1111–8.

Mori C, Spooner ET, Wisniewsk KE, Wisniewski TM, Yamaguch H, Saido TC, et al. Intraneuronal Aβ42 accumulation in Down syndrome brain. Amyloid 2002;9:88–102.

Nishitsuji K, Tomiyama T, Ishibashi K, Ito K, Teraoka R, Lambert MP, et al. The E693Δ mutation in amyloid precursor protein increases intracellular accumulation of amyloid β oligomers and causes endoplasmic reticulum stress-induced apoptosis in cultured cells. Am J Pathol 2009;174:957–69.

Oakley H, Cole SL, Logan S, Maus E, Shao P, Craft J, et al. Intraneuronal beta-amyloid aggregates, neurodegeneration, and neuron loss in transgenic mice with five familial Alzheimer's disease mutations: potential factors in amyloid plaque formation. J Neurosci 2006;26:10129–40.

Oddo S, Caccamo A, Shepherd JD, Murphy MP, Golde TE, Kayed R, et al. Triple-transgenic model of Alzheimer's disease with plaques and tangles: intracellular Aβ and synaptic dysfunction. Neuron 2003;39:409–21.

Oddo S, Caccamo A, Smith IF, Green KN, LaFerla FM. A dynamic relationship between intracellular and extracellular pools of Aβ. Am J Pathol 2006;168:184–94.

Petanceska SS, DeRosa S, Olm V, Diaz N, Sharma A, Thomas-Bryant T, et al. Statin therapy for Alzheimer's disease: will it work? J Mol Neurosci 2002;19:155–61.

Refolo LM, Malester B, LaFrancois J, Bryant-Thomas T, Wang R, Tint GS, et al. Hypercholesterolemia accelerates the Alzheimer's amyloid pathology in a transgenic mouse model. Neurobiol Dis 2000;7:321–31.

Schreurs BG. The effects of cholesterol on learning and memory. Neurosci Biobehav Rev 2010;34:1366–79.

Selkoe DJ. Alzheimer's disease is a synaptic failure. Science 2002;298:789–91.

Shie FS, Jin LW, Cook DG, Leverenz JB, LeBoeuf RC. Diet-induced hypercholesterolemia enhances brain Aβ accumulation in transgenic mice. Neuroreport 2002;13:455–9.

Simons M, Keller P, De Strooper B, Beyreuther K, Dotti CG, Simons K. Cholesterol depletion inhibits the generation of β-amyloid in hippocampal neurons. Proc Natl Acad Sci U S A 1998;95:6460–4.

Solomon A, Kivipelto M. Cholesterol-modifying strategies for Alzheimer's disease. Expert Rev Neurother 2009;9:695–709.

Stefani M, Liguri G. Cholesterol in Alzheimer's disease: unresolved questions. Curr Alzheimer Res 2009;6:15–29.

Takahashi RH, Milner TA, Li F, Nam EE, Edgar MA, Yamaguchi H, et al. Intraneuronal Alzheimer Aβ42 accumulates in multivesicular bodies and is associated with synaptic pathology. Am J Pathol 2002;161:1869–79.

Tampellini D, Capetillo-Zarate E, Dumont M, Huang Z, Yu F, Lin MT, et al. Effects of synaptic modulation on β-amyloid, synaptophysin, and memory performance in Alzheimer's disease transgenic mice. J Neurosci 2010;30:14299–304.

Tomiyama T, Nagata T, Shimada H, Teraoka R, Fukushima A, Kanemitsu H, et al. A new amyloid β variant favoring oligomerization in Alzheimer's-type dementia. Ann Neurol 2008;63:377–87.

Tomiyama T, Matsuyama S, Iso H, Umeda T, Takuma H, Ohnishi K, et al. A mouse model of amyloid β oligomers: their contribution to synaptic alteration, abnormal tau phosphorylation, glial activation, and neuronal loss in vivo. J Neurosci 2010;30:4845–56.

Ullrich C, Pirchl M, Humpel C. Hypercholesterolemia in rats impairs the cholinergic system and leads to memory deficits. Mol Cell Neurosci 2010;45:408–17.

Umeda T, Mori H, Zheng H, Tomiyama T. Regulation of cholesterol efflux by amyloid β secretion. J Neurosci Res 2010;88:1985–94.

Umeda T, Tomiyama T, Sakama N, Tanaka S, Lambert MP, Klein WL, et al. Intraneuronal amyloid β oligomers cause cell death via endoplasmic reticulum stress, endosomal/lysosomal leakage, and mitochondrial dysfunction in vivo. J Neurosci Res 2011;89:1031–42.

Wegenast-Braun BM, Fulgencio Maisch A, Eicke D, Radde R, Herzig MC, Staufenbiel M, et al. Independent effects of intra- and extracellular Aβ on learning-related gene expression. Am J Pathol 2009;175:271–82.

Wirths O, Multhaup G, Bayer TA. A modified β-amyloid hypothesis: intraneuronal accumulation of the β-amyloid peptide – the first step of a fatal cascade. J Neurochem 2004;91:513–20.

Xiong H, Callaghan D, Jones A, Walker DG, Lue LF, Beach TG, et al. Cholesterol retention in Alzheimer's brain is responsible for high β- and γ-secretase activities and Aβ production. Neurobiol Dis 2008;29:422–37.

Neurochemistry International 61 (2012) 347–355

Contents lists available at SciVerse ScienceDirect

Neurochemistry International

journal homepage: www.elsevier.com/locate/nci

Proteomic analysis of the brain tissues from a transgenic mouse model of amyloid β oligomers

Masaoki Takano [a], Kouji Maekura [a], Mieko Otani [a], Keiji Sano [a], Tooru Nakamura-Hirota [b], Shogo Tokuyama [c], Kyong Son Min [d], Takami Tomiyama [e], Hiroshi Mori [e,f], Shogo Matsuyama [b,*]

[a] Department of Life Sciences Pharmacy, School of Pharmaceutical Sciences, Kobe Gakuin University, 1-1-3 Minatojima, Chuo-ku, Kobe 650-8586, Japan
[b] Faculty of Pharmaceutical Sciences, Himeji Dokkyo University, 7-2-1 Kamiohno, Himeji 670-8524, Japan
[c] Department of Clinical Pharmacy, School of Pharmaceutical Sciences, Kobe Gakuin University, 1-1-3 Minatojima, Chuo-ku, Kobe 650-8586, Japan
[d] Laboratory of Toxicology, Faculty of Pharmacy, Osaka Ohtani University, 3-11-1 Nishikigorikita, Tondabayashi, Osaka 584-8540, Japan
[e] Department of Neuroscience and Neurology, Osaka City University Graduate School of Medicine, Osaka 545-8585, Japan
[f] Core Research for Evolutional Science and Technology, Japan Science and Technology Agency, Japan

ARTICLE INFO

Article history:
Received 3 October 2011
Received in revised form 11 May 2012
Accepted 14 May 2012
Available online 23 May 2012

Keywords:
Proteome
Amyloid β oligomers
Alzheimer's disease
Hippocampus
Cortex
Phosphoproteome

ABSTRACT

Amyloid β (Aβ) oligomers are presumed to be one of the causes of Alzheimer's disease (AD). Previously, we identified the E693Δ mutation in amyloid precursor protein (APP) in patients with AD who displayed almost no signals of amyloid plaques in amyloid imaging. We generated APP-transgenic mice expressing the E693Δ mutation and found that they possessed abundant Aβ oligomers from 8 months of age but no amyloid plaques even at 24 months of age, indicating that these mice are a good model to study pathological effects of Aβ oligomers. To elucidate whether Aβ oligomers affect proteome levels in the brain, we examined the proteins and phosphoproteins for which levels were altered in 12-month-old $APP_{E693\Delta}$-transgenic mice compared with age-matched non-transgenic littermates. By two-dimensional gel electrophoresis (2DE) followed by staining with SYPRO Ruby and Pro-Q Diamond and subsequent mass spectrometry techniques, we identified 17 proteins and 3 phosphoproteins to be significantly changed in the hippocampus and cerebral cortex of $APP_{E693\Delta}$-transgenic mice. Coactosin like-protein, SH3 domain-bind glutamic acid-rich-like protein 3 and astrocytic phosphoprotein PEA-15 isoform 2 were decreased to levels less than 0.6 times those of non-transgenic littermates, whereas dynamin, profilin-2, vacuolar adenosine triphosphatase and creatine kinase B were increased to levels more than 1.5 times those of non-transgenic littermates. Furthermore, 2DE Western Blotting validated the changed levels of dynamin, dihydropyrimidinase-related protein 2 (Dpysl2), and coactosin in $APP_{E693\Delta}$-transgenic mice. Glyoxalase and isocitrate dehydrogenase were increased to levels more than 1.5 times those of non-transgenic littermates. The identified proteins could be classified into several groups that are involved in regulation of different cellular functions, such as cytoskeletal and their interacting proteins, energy metabolism, synaptic component, and vesicle transport and recycling. These findings indicate that Aβ oligomers altered the levels of some proteins and phosphoproteins in the hippocampus and cerebral cortex, which could illuminate novel therapeutic avenues for the treatment of AD.

1. Introduction

Alzheimer's disease (AD) is the most frequent neurodegenerative disorder and the most common cause of dementia in the elderly (Lee et al., 2001). AD is neuropathologically characterized by abnormal accumulation of extracellular amyloid plaques and intracellular neurofibrillary tangles throughout cortical and limbic regions. There are numerous, complex pathological changes in AD brain that contribute to neural and synaptic degeneration, including mitochondrial dysfunction, oxidative damage, and inflammation (Akiyama et al., 2000; Glenner and Wong, 1984; Nunomura et al., 2001). Although the current amyloid cascade hypothesis (Hardy and Selkoe, 2002) and tau hypothesis (Lee et al., 2001) provide frameworks for studying AD pathogenesis, the detailed molecular mechanisms that translate amyloid or tau accumulation into neural damage and functional brain impairments are largely unknown. Recently, diverse lines of evidence suggest that amyloid-beta (Aβ) peptides play more important roles in AD pathogenesis (Klein et al., 2001; Li et al., 2009; Selkoe, 2002). Especially, soluble oligomers of Aβ could be a cause of synaptic and cognitive dysfunction in the early stage of AD.

We previously identified the E693Δ mutation in amyloid precursor protein (APP) in patients with AD who displayed almost

* Corresponding author.
E-mail address: shogo@himeji-du.ac.jp (S. Matsuyama).

0197-0186/$ - see front matter © 2012 Elsevier Ltd. All rights reserved.
http://dx.doi.org/10.1016/j.neuint.2012.05.018

no signals of amyloid plaques in amyloid imaging (Tomiyama et al., 2008). To address the relationship between Aβ oligomers and pathological features of AD, we generated APP transgenic mice expressing the E693Δ mutation, which enhanced Aβ oligomerization without fibrillization (Tomiyama et al., 2011). The $APP_{E693\Delta}$-transgenic mice displayed age-dependent accumulation of intraneuronal Aβ oligomers from 8 months and showed impairment of hippocampal synaptic plasticity and memory at 8 months, abnormal tau phosphorylation from 8 months, glial activation from 12–18 months, and neuronal loss at 24 months, but no amyloid plaques even at 24 months (Tomiyama et al., 2011). Thus, the $APP_{E693\Delta}$-transgenic mice might become a useful model to elucidate Aβ oligomer-dependent pathways in AD pathology.

The $APP_{E693\Delta}$-transgenic mouse model might provide a clue for elucidating AD pathology to detect proteomic alteration caused by Aβ oligomers in the brain. One of the most utilized approaches in proteomics to quantify and identify proteins is 2DE and mass spectrometry (MS)(Gorg et al., 2000). This proteomic approach as revealed differential levels of proteins expressed in the brains of AD patients (Sultana et al., 2007), mutant APP transgenic mice (Shin et al., 2004), and mutant tau transgenic mice (Takano et al., 2009). Using the 2DE and MS approach, we identified 17 proteins and 3 phosphoproteins for which levels were altered in the hippocampus and cerebral cortex of 12-month-old $APP_{E693\Delta}$-transgenic mice compared with age-matched non-transgenic littermates. These proteins might play pivotal roles in the early stage of AD.

2. Experimental procedures

2.1. Materials

Sodium dodecyl sulfate, urea, thiourea, CHAPS, dithiothreitol, iodoacetamide, bromo phenol blue, and RNase A and DNase I for SDS–PAGE or 2DE were all obtained from Wako Pure Chemical Industries (Osaka, Japan). Source information for all other assay reagents and materials are incorporated into their respective assay methods described below.

2.2. Animal subjects

Transgenic mice expressing human APP_{695} with the $APP_{E693\Delta}$ mutation under the mouse prion promoter (Tomiyama et al., 2011) were used. Heterozygous human $APP_{E693\Delta}$-transgenic mice and age-matched non-transgenic littermates were sacrificed at 12 months of age, and their hippocampi and cortices were isolated on an ice-cold plate. Animal care and handling were performed strictly in accordance with the Guidelines for Animal Experimentation at Kobe Gakuin University and Himeji Dokkyo University. Every effort was made to minimize the number of animals used and their suffering.

2.3. Sample preparation

The isolated hippocampus and cortex were transferred to a 1.5-ml tube, centrifuged (15,000g, 5 min at 4 °C), resuspended in 100 μl of lysis buffer (7 M urea, 2 M thiourea, 5% CHAPS, 2% IPG buffer [GE Healthcare UK Ltd., England], 50 mM 2-mercaptoethanol, 2.5 μg/ml DNase I, 2.5 μg/ml RNase A), and disrupted by sonication for 30 s. Lysate was again centrifuged (15,000g, 30 min) to remove cellular debris, and the supernatant was recovered for use in 2DE.

2.4. Two-dimensional electrophoresis

2DE was carried out by the method as previously described (Otani et al., 2011) with minor modifications. Approximately 500 μg of protein was applied to ImmobilineDryStrip pH 3–10 NL (7 cm) gels (GE Healthcare UK Ltd., England) and separated at 50 V for 6 h, at 100 V for 6 h, and at 2000 V for 6 h. The immobilised pH gradient (IPG) strips were equilibrated for 15 min in 50 mM Tris/HCl (pH8.8), 6 M urea, 30% (v/v) glycerol, 1% SDS, and 1% (v/v) DTT, and then for 15 min in the same buffer with 2.5% (w/v) iodoacetamide instead of DTT. After equilibration, the IPG strips were set onto a 12.5% acrylamide gel and SDS–polyacrylamide gel electrophoresis was performed at 5 mA/gel for 7 h.

2.5. SYPRO Ruby staining

Proteins on SDS–polyacrylamide gels were detected using the SYPRO Ruby Protein Gel Stain (Molecular Probes). Gels after 2DE were fixed in a solution containing 10% acetic acid/50% methanol for 30 min, then 7% acetic acid/10% methanol for 30 min. After fixing, the gels were incubated in the undiluted stock solution of SYPRO Ruby for 90 min, and destained with 7% acetic acid/10% methanol for 30 min. After rinsing with H_2O for 10 min, digital images were acquired using a Fluorophorestar 3000 image capture system (Anatech, Japan) with 470 nm excitation and 618 nm emission for SYPRO Ruby detection.

2.6. Pro-Q Diamond staining

Phosphoproteins on SDS–polyacrylamide gels were detected using Pro-Q Diamond Phosphoprotein Stain (Molecular Probes). Gels after 2DE were fixed in a solution containing 10% acetic acid/50% methanol for 30 min two times, and then the gels were washed with MilliQ H_2O for 10 min twice. The gels were then incubated in an undiluted stock solution of Pro-Q Diamond for 90 min, and destained with three successive washes (30 min per wash) in 50 mM sodium acetate (pH 4.0), 20% (v/v) acetonitrile. Digital images were acquired using the Fluorophorestar 3000 image capture system with 520 nm excitation and 575 nm emission for Pro-Q Diamond detection.

2.7. Image analysis

Following image acquisition, 2D gel imaging and analysis software Prodigy SameSpots (Nonlinear Dynamics, UK) version 1.0 was used for gel-to-gel matching and identifying differences between non-transgenic and mutant APP transgenic mouse samples. Each of five sets of samples was represented by two independent gels biological replicates of 2DE gels. The gel images were normalized in the Prodigy SameSpots software to even out differences in staining intensities among gels. ANOVA was performed with 95% significance level to determine which proteins were differentially expressed between the non-transgenic and mutant APP transgenic mice. A minimum of 1.3-fold change was considered to identify the increased proteins and 0.7-fold change for decreased proteins.

2.8. In-gel digestion and peptide extraction

In-gel digestion was performed in accordance with the method of (Yokoyama et al., 2004). Protein spots in the gels stained with SYPRO Ruby or Pro-Q Diamond were cut out and subjected to trypsin digestion with porcine trypsin (Promega, Madison, WI, USA). Briefly, gel pieces were washed, dehydrated, and diluted in 200 μl of 25 mM ammonium hydrogen carbonate with 5% ACN

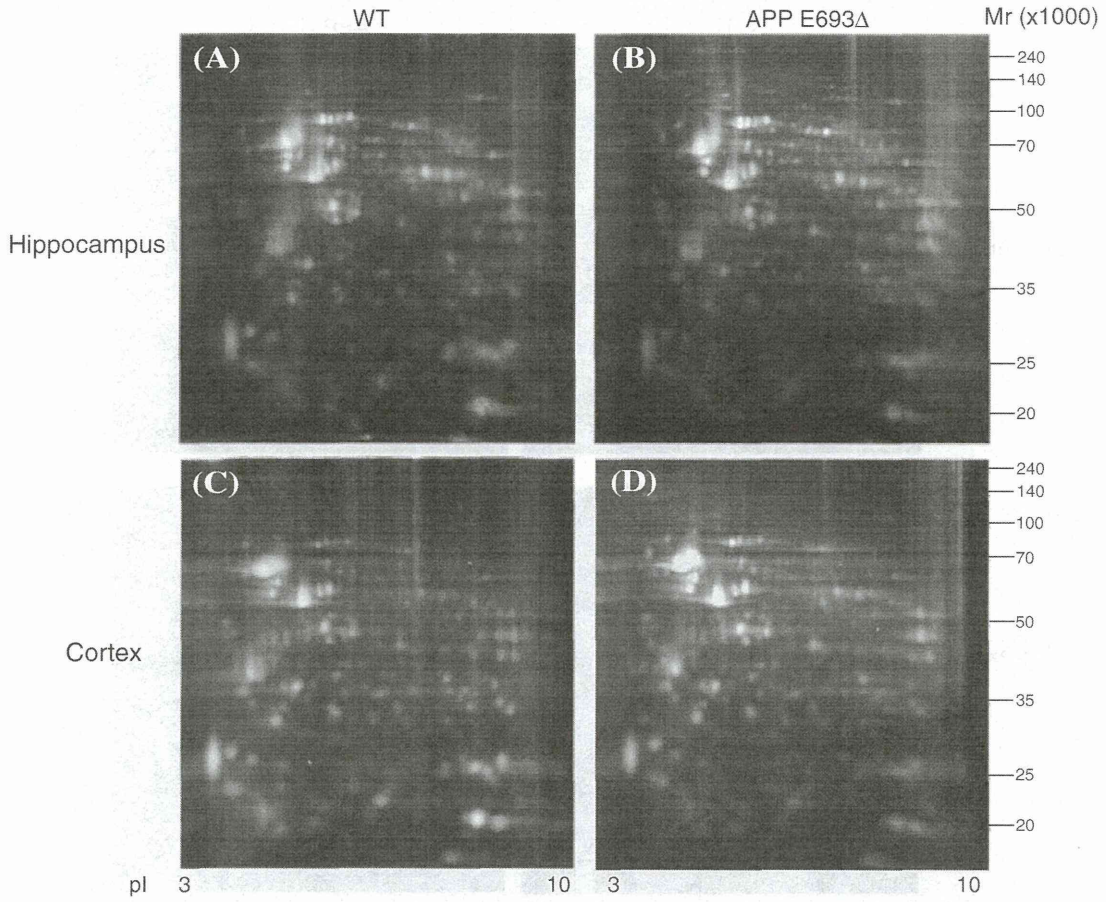

Fig. 1. SYPRO Ruby-stained 2DE gels (pH range 3–10) for the hippocampus and cerebral cortex from non-transgenic and $APP_{E693\Delta}$-transgenic mice. To each gel, 500 μg of protein was loaded for detection of protein expression. (A) Hippocampus of wild-type (or non-transgenic) littermates, (B) hippocampus of $APP_{E693\Delta}$-transgenic mice, (C) cortex of wild-type (or non-transgenic) littermates and (D) cortex of $APP_{E693\Delta}$-transgenic mice. Protein molecular mass standards (*y*-axis) and pHs (*x*-axis) are shown.

(v/v). Trypsin (5 μl, 10 ng/μl) was added and the digestion was incubated for 10 h at 37 °C. After separation of supernatant, gel pieces were washed again and then extracted with 50/50 ACN/0.3% (v/v) trifluoroacetic acid for 10 min by sonication. The supernatant was once again collected, mixed with the two fractions, and evaporated under vacuum. The extracted peptides were then diluted in 5 μl of 50/50 ACN/0.3% (v/v) trifluoroacetic acid.

2.9. Mass spectrometry analysis and protein identification

Mass spectra were recorded in positive reflection mode using a MALDI-TOF MS/MS analyzer (ABI PLUS 4800, Applied Biosystems), equipped with a delayed ion technology. The samples were dissolved in 5 μl of 50/50 ACN/0.3% (v/v) trifluoroacetic acid. For the matrix, α-cyano-4-hydroxycinnamic acid (1 μg/μl: Wako Junyaku, Osaka, Japan) dissolved in the same mixture was used. Analyte and matrix were spotted consecutively in a 1:1 ratio on a stainless steel target and dried under ambient conditions. All spectra acquired by MALDI-TOF MS were externally calibrated with peptide calibration standard II (Bruker Daltonics, Germany). An MS condition of 2500 shots per spectrum was used. Automatic monoisotopic precursor selection for MS/MS was done using an interpretation method based on the 12 most intense peaks per spot with an MS/MS mode condition of 4000 laser shots per spectrum. Minimum peak width was one fraction and mass tolerance was 80 ppm. Adduct tolerance was (m/z) ± 0.003. MS/MS was performed with a gas pressure of 1×10^{-6} bar in the collision cell. Ambient air was used as collision gas. Data analyses were performed using Data Explorer version 4.9 (Applied Biosystems) software, and proteins were identified through the search engine Mascot (www.matrixscience.com; Matrix Science, Boston, MA) (peptide mass tolerance: 60 ppm; MS/MS tolerance: 0.3 Da; maximum missed cleavages: 1) using the protein database NCBInr. Proteins identified by MALDI-TOF MS with a score of 79 or higher were considered significant ($p < 0.05$). Single peptides identified by MALDI–TOF/TOF MS/MS with individual ions scores greater than 47 indicate identity or extensive homology ($p < 0.05$).

2.10. 2DE Western Blotting

Approximately 100 μg of protein from mouse hippocampus was applied to ImmobilineDryStrip pH 3–10 NL (7 cm) gel in first dimension, and then the IPG strips were set onto a 10.0% acrylamide gel and SDS–polyacrylamide gel electrophoresis was performed at 5 mA/gel for 7 h in second dimension. The gels were transferred onto PVDF membranes (Pall Corporation, Pensacola, FL, USA), in a trans-blot electrophoresis transfer cell (Nihon Eido, Tokyo, Japan). Western Blotting were performed by using monoclonal antibodies against dynamin (diluted 1:1000, Cell Signaling, USA), polyclonal antibodies Dpysl2, coactosin and voltage-dependent anion-selective channel protein 1 (VDAC) (diluted 1:1000, Cell Signaling, USA). Peroxidase-conjugated antibody (diluted 1:5000, Abcam, USA) was used as secondary antibody. The reaction was detected by chemiluminescence with ECL reagents (Pierce Biotechnology, USA). A semi quantitative analysis based on optical density was

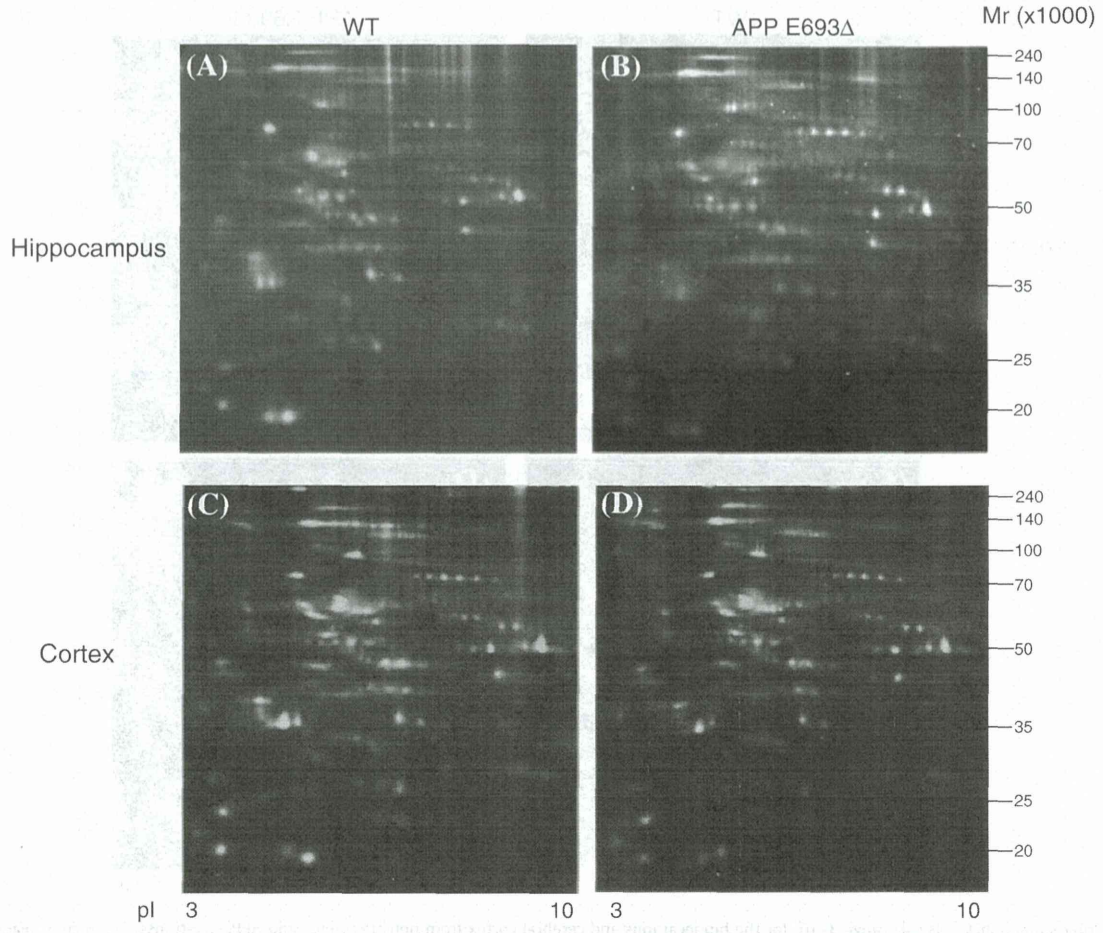

Fig. 2. Pro-Q Diamond-stained 2DE gels for the hippocampus and cerebral cortex from non-transgenic and $APP_{E693\Delta}$-transgenic mice. To each gel, 500 μg of protein was loaded for detection of protein expression. (A) Hippocampus of wild-type (or non-transgenic) littermates, (B) hippocampus of $APP_{E693\Delta}$-transgenic mice, (C) cortex of wild-type (or non-transgenic) littermates and (D) cortex of $APP_{E693\Delta}$-transgenic mice. Protein molecular mass standards (*y*-axis) and pHs (*x*-axis) are shown.

performed by ImageJ software (available at http://www.rsbweb.nih.gov/ij).

3. Results

The levels of proteins and phosphoproteins in the hippocampus and cerebral cortex of $APP_{E693\Delta}$-transgenic mice were compared to those of non-transgenic littermates. The altered levels of proteins and phosphoproteins were quantified and identified from 2DE gels using Prodigy SameSpots software for MALDI–MS/MS. We showed representative 2DE gels stained with SYPRO Ruby and Pro-Q Diamond for the hippocampus and cerebral cortex of non-transgenic mice and $APP_{E693\Delta}$-transgenic mice (Figs. 1 and 2) and the raw data for the reproducibility of 2DE gels (Supplementary Fig. 1A–D). There were approximately 350 spots in each SYPRO Ruby-stained 2DE gel from hippocampus and cortex of WT and $APP_{E693\Delta}$-transgenic mice (Fig. 1A-D), and approximately 270 spots in each ProQ Diamond-stained 2DE gel from hippocampus and cortex of WT and $APP_{E693\Delta}$-transgenic mice (Fig. 2A-D). The indicated spots of 2DE gels showed altered levels of proteins (Fig. 3), for which spots were excised according to the Prodigy program. Comparing the intensity of protein spots from the hippocampus and cerebral cortex of $APP_{E693\Delta}$-transgenic mice to those of non-transgenic mice, the levels of 70 protein spots (ANOVA < 0.05, fold > 1.3 or <0.7) and 17 phosphoprotein spots (ANOVA < 0.05, fold > 1.3 or <0.7) were altered. Finally, the total 22 polypeptides were identified, including 15 polypeptides in SYPRO Ruby-stained gel from hippocampus (Table 1), 7 polypeptides in SYPRO Ruby-stained gel from cortex (Table 2), and 3 polypeptides in ProQ Diamond-stained gel from hippocampus (Table 3). We also showed the raw data of spot intensities about the reproducibility of their bioinformatic analysis (Supplementary Fig. 2A–C).

3.1. Identification of altered proteins in $APP_{E693\Delta}$-transgenic mice hippocampus

Protein levels were significantly decreased for coactosin-like protein, SH3 domain-bind glutamic acid-rich-like protein3, astrocytic phosphoprotein PEA-15 isoform 2, dual specificity protein phosphatase 3, and phosphatidylethanolamine-binding protein, and increased for dynamin, profilin-2, vacuolar adenosine triphosphatase subunit B, transketolase, Dpysl2, Atp5b protein and fascin in the hippocampus (Table 1). To benchmark the proteomic analysis, we chose VDAC and MDH 2 as common, non-regulated proteins. Protein levels of VDAC and MDH 2 were not changed in the hippocampus of $APP_{E693\Delta}$-transgenic mice, compared to non-transgenic mice (Table 1).

3.2. Identification of altered proteins in $APP_{E693\Delta}$-transgenic mice cortex

Protein levels were significantly decreased for profilin-2, LMW phosphotyrosine protein phosphatase isoform 2, coactosin-like